

χ_{cJ} production at hadron colliders with QCD radiative corrections

Yan-Qing Ma ^(a), Kai Wang ^(a), and Kuang-Ta Chao ^(a,b)

(a) Department of Physics and State Key Laboratory of Nuclear Physics and Technology, Peking University, Beijing 100871, China
 (b) Center for High Energy Physics, Peking University, Beijing 100871, China

To confront the outstanding problem in χ_{cJ} hadroproduction that at the Tevatron the observed ratio of cross sections $R_{\chi_c} = \sigma_{\chi_{c2}}/\sigma_{\chi_{c1}} \approx 0.75$ at large p_T is much smaller than the predicted value $5/3$ at leading-order (LO) in nonrelativistic QCD (NRQCD), we find large but, crucially, negative contributions scaling as $1/p_T^4$ from the color-singlet ${}^3P_J^{[1]} (J=0,1,2)$ channels at next-to-leading order (NLO) in α_s , while other higher order contributions at large p_T are suppressed. As a result, by introducing one color-octet matrix element $\langle \mathcal{O}^{\chi_{c0}}({}^3S_1^{[8]}) \rangle = 2.2 \times 10^{-3} \text{ GeV}^3$ with one known color-singlet matrix element, we can naturally fit the observed ratio R_{χ_c} and predict the χ_{cJ} production cross sections at the Tevatron and LHC, which clearly shows that a sizable color-octet contribution is needed in the P-wave charmonium production. Feeddown contributions of χ_{cJ} to prompt J/ψ production are estimated to be substantial, e.g. $30 - 40\%$ at $p_T = 20 \text{ GeV}$ at the Tevatron.

PACS numbers: 12.38.Bx, 13.25.Gv, 14.40.Gx

Heavy quarkonium production remains a challenging problem in understanding quantum chromodynamics. Among others, the puzzle of $J/\psi(\psi')$ production cross sections and polarizations at large transverse momentum p_T at the Tevatron is crucial in testing the color-octet (CO) and color-singlet (CS) mechanisms in NRQCD[1] and other mechanisms (for reviews see e.g.[2]). The P-wave charmonia χ_{cJ} ($J=0,1,2$) production is equally important, since they give substantial feeddown contributions to the prompt J/ψ production through decays $\chi_{cJ} \rightarrow \gamma J/\psi$. An even more important issue in χ_{cJ} production concerns the ratio of production rates of χ_{c2} to χ_{c1} . The CDF Collaboration measured the ratio

$$R_{\chi_c} = \sigma_{\chi_{c2}}/\sigma_{\chi_{c1}} \quad (1)$$

to be about 0.75 for $p_T > 4 \text{ GeV}$, and even smaller when p_T becomes larger[3]. But at LO in α_s , NRQCD predicts the χ_c production cross sections to scale as $1/p_T^6$ in the CS ${}^3P_J^{[1]}$ channels while scale as $1/p_T^4$ in the CO ${}^3S_1^{[8]}$ channel. Thus ${}^3S_1^{[8]}$ would dominate at large p_T , predicting the ratio to be $5/3$ by spin counting[4, 5]. This prediction is much larger than the measured value 0.75.

In recent years the NLO QCD corrections have been found to be essential in charmonium production. The large discrepancies between experiments and LO predictions (see e.g. [6]) for J/ψ exclusive and inclusive production in e^+e^- annihilation at B factories can be largely resolved at NLO within CS channels[7]. For J/ψ photoproduction at HERA, complete NLO calculations[8] slightly favor the presence of CO contributions. For the J/ψ production at the Tevatron, the NLO correction in CS channels enhances the cross section at large p_T by two orders of magnitude [9, 10]. So, a crucial issue in charmonium production seems to be whether the CO contributions are still needed in NRQCD.

Here we will study the NLO QCD corrections to the χ_{cJ} production. Our aim is to clarify the puzzle of χ_{cJ}

ratio R_{χ_c} , predict the χ_{cJ} production cross sections at the Tevatron and LHC, and estimate the χ_{cJ} feeddown contribution to the prompt J/ψ production. Our study will also shed light on the quarkonium production mechanisms especially the CO mechanism in NRQCD.

In NRQCD the inclusive cross section for the direct χ_{cJ} production in hadron-hadron collisions is given by

$$\begin{aligned} d\sigma[pp \rightarrow \chi_{cJ} + X] &= \sum_n \hat{d}\sigma[(c\bar{c})_n] \frac{\langle \mathcal{O}_n^{\chi_{cJ}} \rangle}{m_c^{2L_n}} \quad (2) \\ &= \sum_{i,j,n} \int dx_1 dx_2 G_{i/p} G_{j/p} \times \hat{d}\sigma[i + j \rightarrow (c\bar{c})_n + X] \langle \mathcal{O}_n^{\chi_{cJ}} \rangle, \end{aligned}$$

where p is either a proton or an antiproton, the indices i, j run over all the partonic species and n denotes the color, spin and angular momentum (L_n) of the intermediate $c\bar{c}$ pair. In this work, we calculate the cross sections at NLO in α_s and LO in v (the relative velocity of quark and antiquark). So only two channels ${}^3P_J^{[1]}$ and ${}^3S_1^{[8]}$ in the present calculation are involved. The long-distance-matrix elements (LDMEs) $\langle \mathcal{O}_n^{\chi_{cJ}} \rangle$ are related to the transition probabilities from the intermediate state $(c\bar{c})_n$ into χ_{cJ} , and are governed by the non-perturbative QCD dynamics. Note that our definition of CS LDMEs $\langle \mathcal{O}^{\chi_{cJ}}({}^3P_J^{[1]}) \rangle$ are different from that in Ref.[1] by a factor of $1/(2N_c)$. And $\langle \mathcal{O}^{\chi_{cJ}}({}^3P_J^{[1]}) \rangle$ ($J=0,1,2$) are related to just one matrix element by spin symmetry.

We use **FeynArts**[12] to generate Feynman diagrams and amplitudes. Some representative diagrams are shown in Fig. 1. There are generally ultraviolet (UV), infrared (IR) and Coulomb singularities. Conventional dimensional regularization (CDR) with $D = 4 - 2\epsilon$ is adopted to regularize them. We have checked analytically that all singularities are canceled exactly. The UV divergences from self-energy and triangle diagrams are removed by renormalization.

The renormalization constants Z_m, Z_2, Z_{2l} and Z_3 ,

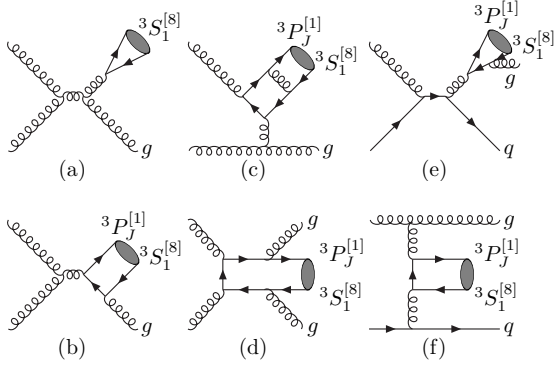


FIG. 1: Representative Feynman diagrams for χ_{cJ} hadroproduction at LO and NLO. The gluon-gluon and gluon-quark subprocesses are all included. In (b)-(f) both color-singlet ${}^3P_J^{[1]}$ and color-octet ${}^3S_1^{[8]}$ channels contribute.

which correspond, respectively, to the charm quark mass m_c , charm-field ψ_c , light quark field ψ_q and gluon field A_μ^a are defined in the on-mass-shell(OS) scheme, while Z_g corresponding to the QCD gauge coupling α_s is defined in the modified-minimal-subtraction($\overline{\text{MS}}$) scheme:

$$\begin{aligned}
 \delta Z_m^{OS} &= -3C_F \frac{\alpha_s}{4\pi} N_\epsilon \left[\frac{1}{\epsilon_{UV}} + \frac{4}{3} \right], \\
 \delta Z_2^{OS} &= -C_F \frac{\alpha_s}{4\pi} N_\epsilon \left[\frac{1}{\epsilon_{UV}} + \frac{2}{\epsilon_{IR}} + 4 \right], \\
 \delta Z_{21}^{OS} &= -C_F \frac{\alpha_s}{4\pi} N_\epsilon \left[\frac{1}{\epsilon_{UV}} - \frac{1}{\epsilon_{IR}} \right], \\
 \delta Z_3^{OS} &= \frac{\alpha_s}{4\pi} N_\epsilon \left[(\beta_0(n_f) - 2C_A) \left(\frac{1}{\epsilon_{UV}} - \frac{1}{\epsilon_{IR}} \right) \right], \\
 \delta Z_g^{\overline{\text{MS}}} &= -\frac{\beta_0(n_f)}{2} \frac{\alpha_s}{4\pi} N_\epsilon \left[\frac{1}{\epsilon_{UV}} + \ln \frac{m_c^2}{\mu^2} \right], \quad (3)
 \end{aligned}$$

where $N_\epsilon = \left(\frac{4\pi\mu^2}{m_c^2} \right)^\epsilon \Gamma(1+\epsilon)$ is a overall factor in our calculation, $\beta_0(n_f) = \frac{11}{3}C_A - \frac{4}{3}T_F n_f$ is the one-loop coefficient of the QCD beta function, $n_f = 3$ is the number of active quark flavors and μ is the renormalization scale.

IR singularities arising from loop integration and phase space integration of the real correction partially cancel each other. The remaining singularities of the S-wave state ${}^3S_1^{[8]}$ are absorbed by the proton parton-distribution-functions (PDFs), while that of ${}^3P_J^{[1]}$ states are absorbed by both the proton PDFs and $\langle \mathcal{O}^{\chi_{c0}}({}^3S_1^{[8]}) \rangle$. We extract poles in the real corrections using the phase space slicing method[13]. We note that to correctly get the soft poles, the eikonal current should be taken before the heavy quarks are coupled to states with definite quantum numbers. We can verify that our results are independent of the two cuts introduced in the phase space slicing for each subgroup associated with a real correction process.

There are thousands of diagrams which are handled by our self-written `Mathematica` program and then changed

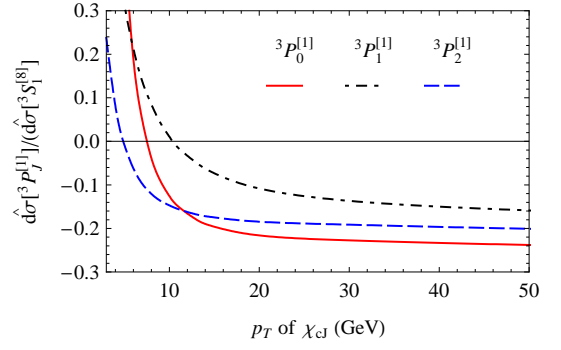


FIG. 2: The ratio of $\hat{d}\sigma[{}^3P_J^{[1]}]$ to $\hat{d}\sigma[{}^3S_1^{[8]}]$ as a function of p_T at the Tevatron. The cut $|y_{\chi_{cJ}}| < 1$ is chosen to compare with the CDF data of Ref. [3].

into `C++` code to perform convolution and phase space integration. To perform the calculation, two different methods are used, resulting in two independent computer codes. In one of our methods, the virtual corrections are calculated numerically and using `QCDLoop`[14] to separate the singularities and finite result, while the real corrections are calculated using the helicity method. In the second method, we expand the singularities analytically and use `LoopTools`[15] to get the finite result, while the real corrections are calculated by directly squaring the amplitudes. Results of the two methods are found to coincide with each other.

Essentially, in our calculation the most complicated part is the loop-correction for P-wave channels, where the derivation of the amplitude with respect to the relative momentum of heavy quarks Q and \bar{Q} is involved. This derivation is equivalent to have one additional massive vector boson in the calculation, which causes complicated tensor loop integrals and entangled pattern of infrared (IR) singularities. Using the result in Ref.[11], we developed a new method for loop-integrals, which aims at NLO calculation with bound states. This method makes the NLO QCD corrections for P-wave heavy quarkonium hadroproduction become possible. The details of our method will be presented elsewhere.

Thanks to the LHAPDF interface[16], the CTEQ6L1 and CTEQ6M PDFs are used for LO and NLO calculations respectively. The charm quark mass is set to be $m_c = 1.5$ GeV, while the renormalization, factorization, and NRQCD scales are $\mu_r = \mu_f = m_T$ and $\mu_\Lambda = m_c$, where $m_T = \sqrt{p_T^2 + 4m_c^2}$ is the χ_{cJ} transverse mass. The center-of-mass energies are 1.96 TeV at the Tevatron and 14 TeV at the LHC.

We begin our numerical analysis by comparing the short distance coefficients $\hat{d}\sigma[{}^3P_J^{[1]}]$ of the ${}^3P_J^{[1]}$ channels and $\hat{d}\sigma[{}^3S_1^{[8]}]$ of the ${}^3S_1^{[8]}$ channel at NLO. We find that at NLO the most significant change is the large p_T behavior in the ${}^3P_J^{[1]}$ channels: it scales as $1/p_T^4$ at large p_T at NLO, in contrast to $1/p_T^6$ at LO. As shown in Fig. 2, at LO the ${}^3P_J^{[1]}$ channels are negligible at high p_T , whereas

at NLO the ${}^3P_J^{[1]}$ channels are comparable to the ${}^3S_1^{[8]}$ channel even at $p_T \approx 50$ GeV. Another important but unique feature is that the ${}^3P_J^{[1]}$ channels give large values at high p_T , but surprisingly with negative signs. We note that the negative values are not caused by the choice of μ_Λ , though this may affect their absolute values. In fact, detailed investigation reveals that the negative values are originated from the Subtraction Scheme (SS) for renormalizing the NRQCD LDMEs $\langle \mathcal{O}^{\chi_{c0}}({}^3S_1^{[8]}) \rangle$. The SS in this work is the conventional $\overline{\text{MS}}$ scheme. One may use other SS to get different values of $d\hat{\sigma}[P_J^{[1]}]$, but this should not change the physical result, because the SS dependence of short-distance coefficients of ${}^3P_J^{[1]}$ are canceled by the SS dependence of $\langle \mathcal{O}^{\chi_{c0}}({}^3S_1^{[8]}) \rangle$, and the final physical results are independent of the choice of SS. Especially, $d\sigma[\chi_{cJ}]$ and R_{χ_c} are independent of the SS and μ_Λ , and their values should always be positive.

From Fig. 2 we see that the ${}^3P_1^{[1]}$ channel decreases slower than the ${}^3P_2^{[1]}$ channel. Considering that ${}^3P_J^{[1]}$ channels are comparable to the ${}^3S_1^{[8]}$ channel at high p_T , we may naturally explain the CDF data[3] that the production rate of χ_{c1} exceeds that of χ_{c2} at high p_T . We define the ratio

$$r = \frac{\langle \mathcal{O}^{\chi_{c0}}({}^3S_1^{[8]}) \rangle}{\langle \mathcal{O}^{\chi_{c0}}({}^3P_J^{[1]}) \rangle / m_c^2} \Big|_{\overline{\text{MS}}, \mu_\Lambda = m_c}. \quad (4)$$

The bound of $r > 0.24$ is needed to get a positive production rate of χ_{c0} at high p_T , as shown in Fig. 2. With this definition, we can give an asymptotic expression of R_{χ_c} at the Tevatron with $|y_{\chi_{cJ}}| < 1$:

$$R_{\chi_c} = \frac{5 r d\hat{\sigma}[{}^3S_1^{[8]}] + d\hat{\sigma}[{}^3P_2^{[1]}]}{3 r d\hat{\sigma}[{}^3S_1^{[8]}] + d\hat{\sigma}[{}^3P_1^{[1]}}} \rightarrow \frac{5 r - 0.20}{3 r - 0.16}, \quad (5)$$

where the numbers -0.20 and -0.16 can be read from Fig. 2. With these two numbers, R_{χ_c} must be smaller than $5/3$ at high p_T . By fitting the data [3], we get $r = 0.27 \pm 0.06$, which is compatible with the naive velocity scaling rule $r \approx 1$ [1]. In the fitting procedure, the mass difference between χ_{cJ} and J/ψ is considered. As shown in Fig. 3, the NLO predictions present a much better compatibility with the experiment data than LO, where r is constrained by $0.24 < r < 0.33$ and $R_{J/\psi\gamma} \equiv \mathcal{B}(\chi_{c1} \rightarrow J/\psi\gamma)/\mathcal{B}(\chi_{c2} \rightarrow J/\psi\gamma) = 1.91$ as in Ref. [3].

In Fig. 4, we show predictions for R_{χ_c} at the LHC, where the cut $|y_{\chi_{cJ}}| < 3$ is chosen. Note that, the ratio R_{χ_c} is sensitive to r at NLO. Thus measurement of R_{χ_c} at high p_T will give a strict constraint on r .

To predict the production cross sections, we still need to fix the CS matrix element $\langle \mathcal{O}^{\chi_{c0}}({}^3P_J^{[1]}) \rangle$. As a widely adopted choice, we take the potential model result $|R'_P(0)|^2 = 0.075 \text{ GeV}^5$ (see the B-T model in [17]) as our input parameter. The prediction for χ_{cJ} production at the LHC is presented in Fig. 5, where $r = 0.27$ and $|y_{\chi_{cJ}}| < 3$ are chosen. The p_T spectrum of χ_{cJ} production at the Tevatron has a similar

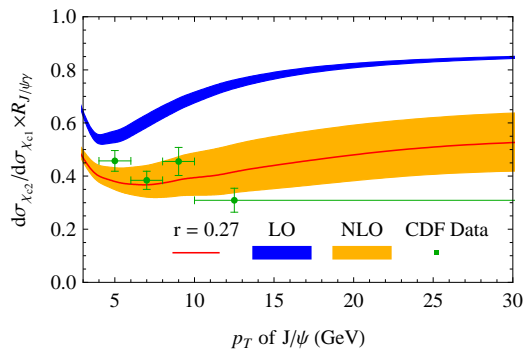


FIG. 3: Transverse momentum distribution of ratio $R_{\chi_c} R_{J/\psi\gamma}$ at the Tevatron with cut $|y_{\chi_{cJ}}| < 1$. The CDF data is taken from Ref.[3], where p_T of χ_c is approximately identified with the measured p_T of J/ψ associated with a photon. The lower and upper bounds of LO and NLO are constrained by $0.24 < r < 0.33$.

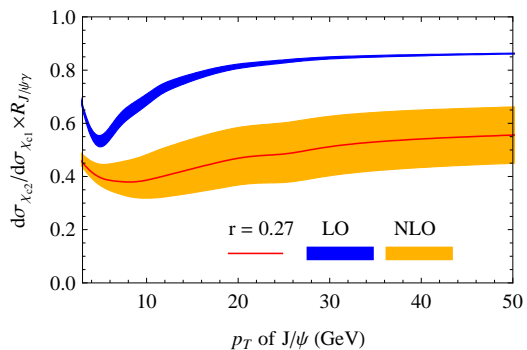


FIG. 4: Transverse momentum distribution of ratio $R_{\chi_c} R_{J/\psi\gamma}$ at the LHC with cut $|y_{\chi_{cJ}}| < 3$. The lower and upper bounds of LO and NLO are constrained by $0.24 < r < 0.33$.

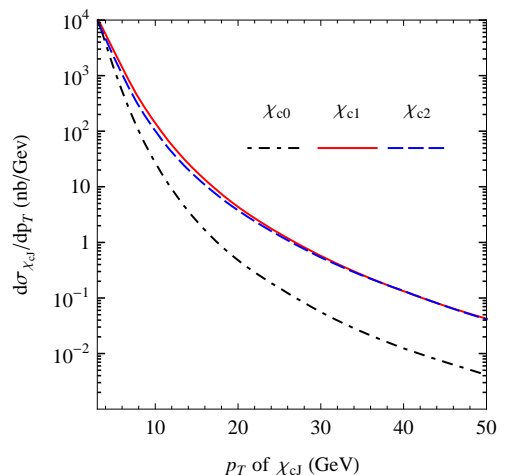


FIG. 5: Transverse momentum distribution of χ_{cJ} production at the LHC with cut $|y_{\chi_{cJ}}| < 3$.

shape to that at the LHC. Furthermore, one can get the χ_{cJ} feeddown contributions to J/ψ by multiplying each state by its decay branching ratio into J/ψ . At the Tevatron, the feeddown contribution has a rather large proportion of the total J/ψ production cross section. If we choose $r = 0.24(0.27)$, the proportion is 25(30)% at $p_T = 10$ GeV, and reaches to about 30(40)% at $p_T = 20$ GeV. Due to this large proportion, χ_{cJ} feed-down will have an important effect on J/ψ polarization in J/ψ prompt production, and should be further clarified when dealing with the J/ψ polarization puzzle.

In summary, we calculate NLO contributions in α_s to χ_{cJ} production at the Tevatron and LHC, including both CS and CO channels. Large contributions of ${}^3P_J^{[1]}$ channels at high p_T are found, but crucially with negative signs. Because ${}^3P_J^{[1]}$ contributions are comparable to that of ${}^3S_1^{[8]}$ at high p_T , and ${}^3P_1^{[1]}$ decreases slower than ${}^3P_2^{[1]}$, the measured ratio of R_{χ_c} at the Tevatron can be naturally explained. By fitting the Tevatron data, we extract the ratio of CO to CS matrix element to be $r = 0.27_{-0.03}^{+0.06}$, where the $\overline{\text{MS}}$ scheme is used and $\mu_\Lambda = m_c$. Choosing a widely used CS matrix element, we predict the production rates of χ_{cJ} at the Tevatron and LHC, which may

also be used to predict the prompt J/ψ production and shed light on the J/ψ polarization puzzle. We emphasize that in χ_{cJ} production the NLO corrections already scale as $1/p_T^4$, which is the leading p_T behavior in this process, and the NNLO and other corrections are no longer important, because they are suppressed either by α_s or by v^2 relative to NLO contributions. This differs markedly from J/ψ production, where NNLO corrections could be even more important than NLO at large p_T [18]. As a result, we have picked up the most important contributions in χ_{cJ} production at large p_T , and therefore given a good description for this process. This work systematically presents $1/p_T^4$ behavior for all important channels in charmonium hadroproduction, gives strong support to the color-octet mechanism, and provides further tests for NRQCD and heavy quakonium production mechanism.

We thank C. Meng and Y.J. Zhang for helpful discussions, and B. Gong and J.X. Wang for useful communications. This work was supported by the National Natural Science Foundation of China (No.10721063) and the Ministry of Science and Technology of China (No.2009CB825200).

-
- [1] G. T. Bodwin, E. Braaten and G. P. Lepage, Phys. Rev. D **51**, 1125 (1995) [Erratum-ibid. D **55**, 5853 (1997)].
- [2] N. Brambilla *et al.*, hep-ph/0412158; J. P. Lansberg, Int. J. Mod. Phys. A **21**, 3857 (2006); J. P. Lansberg *et al.*, arXiv:0807.3666.
- [3] A. Abulencia *et al.* [CDF Collaboration], Phys. Rev. Lett. **98**, 232001 (2007).
- [4] P. L. Cho and A. K. Leibovich, Phys. Rev. D **53**, 150 (1996).
- [5] B. A. Kniehl, G. Kramer and C. P. Palisoc, Phys. Rev. D **68**, 114002 (2003).
- [6] E. Braaten and J. Lee, Phys. Rev. D **67**, 054007 (2003); K. Y. Liu, Z. G. He and K. T. Chao, Phys. Lett. B **557**, 45(2003), Phys. Rev. D **77**, 014002 (2008); K. Hagiwara, E. Kou and C. F. Qiao, Phys. Lett. B **570**, 39 (2003).
- [7] Y. J. Zhang, Y. J. Gao and K. T. Chao, Phys. Rev. Lett. **96**, 092001 (2006); Y. J. Zhang and K. T. Chao, Phys. Rev. Lett. **98**, 092003 (2007); B. Gong and J. X. Wang, Phys. Rev. D **77**, 054028 (2008); B. Gong and J. X. Wang, Phys. Rev. D **80**, 054015 (2009); Y. Q. Ma, Y. J. Zhang and K. T. Chao, Phys. Rev. Lett. **102**, 162002 (2009); B. Gong and J. X. Wang, Phys. Rev. Lett. **102**, 162003 (2009).
- [8] M. Butenschoen and B. A. Kniehl, Phys. Rev. Lett. **104**, 072001 (2010); P. Artoisenet, J. M. Campbell, F. Maltoni and F. Tramontano, Phys. Rev. Lett. **102**, 142001 (2009). C. H. Chang, R. Li and J. X. Wang, Phys. Rev. D **80**, 034020 (2009).
- [9] J. M. Campbell, F. Maltoni and F. Tramontano, Phys. Rev. Lett. **98**, 252002 (2007).
- [10] B. Gong and J. X. Wang, Phys. Rev. Lett. **100**, 232001 (2008); Phys. Rev. D **78**, 074011 (2008).
- [11] A. I. Davydychev, Phys. Lett. B **263**, 107 (1991).
- [12] T. Hahn, Comput. Phys. Commun. **140**, 418 (2001).
- [13] B. W. Harris and J. F. Owens, Phys. Rev. D **65**, 094032 (2002).
- [14] R. K. Ellis and G. Zanderighi, JHEP **0802**, 002 (2008).
- [15] T. Hahn and M. Perez-Victoria, Comput. Phys. Commun. **118**, 153 (1999).
- [16] M. R. Whalley, D. Bourilkov and R. C. Group, arXiv:hep-ph/0508110.
- [17] E. J. Eichten and C. Quigg, Phys. Rev. D **52**, 1726 (1995).
- [18] P. Artoisenet, J. M. Campbell, J. P. Lansberg, F. Maltoni and F. Tramontano, Phys. Rev. Lett. **101**, 152001 (2008); J. P. Lansberg, Eur. Phys. J. C **61**, 693 (2009).